Journal of Magnetic Resonance 260 (2015) 89–97

Contents lists available at ScienceDirect

Journal of Magnetic Resonance

journal homepage: www.elsevier.com/locate/jmr

The use of a selective saturation pulse to suppress t_1 noise in two-dimensional ^{1}H fast magic angle spinning solid-state NMR spectroscopy

Aiden J. Robertson [a,b], Manoj Kumar Pandey [c], Andrew Marsh [b], Yusuke Nishiyama [c,d], Steven P. Brown [a,*]

[a] Department of Physics, University of Warwick, Coventry CV4 7AL, United Kingdom
[b] Department of Chemistry, University of Warwick, Coventry CV4 7AL, United Kingdom
[c] RIKEN CLST-JEOL Collaboration Centre, Yokohama, Kanagawa 230-0045, Japan
[d] JEOL RESONANCE Inc., Musashino, Akishima, Tokyo 196-8558, Japan

ARTICLE INFO

Article history:
Received 27 May 2015
Revised 1 September 2015
Available online 16 September 2015

Keywords:
^{1}H two-dimensional solid-state NMR
DNA based analogue
Selective saturation pulse
t_1 noise
Fast MAS

ABSTRACT

A selective saturation pulse at fast magic angle spinning (MAS) frequencies (60+ kHz) suppresses t_1 noise in the indirect dimension of two-dimensional ^{1}H MAS NMR spectra. The method is applied to a synthetic nucleoside with an intense methyl ^{1}H signal due to triisopropylsilyl (TIPS) protecting groups. Enhanced performance in terms of suppressing the methyl signal while minimising the loss of signal intensity of nearby resonances of interest relies on reducing spin diffusion – this is quantified by comparing two-dimensional ^{1}H NOESY-like spin diffusion spectra recorded at 30–70 kHz MAS. For a saturation pulse centred at the methyl resonance, the effect of changing the nutation frequency at different MAS frequencies as well as the effect of changing the pulse duration is investigated. By applying a pulse of duration 30 ms and nutation frequency 725 Hz at 70 kHz MAS, a good compromise of significant suppression of the methyl resonance combined with the signal intensity of resonances greater than 5 ppm away from the methyl resonance being largely unaffected is achieved. The effectiveness of using a selective saturation pulse is demonstrated for both homonuclear ^{1}H–^{1}H double quantum (DQ)/single quantum (SQ) MAS and ^{14}N–^{1}H heteronuclear multiple quantum coherence (HMQC) two-dimensional solid-state NMR experiments.

1. Introduction

Two-dimensional homonuclear and heteronuclear ^{1}H solid-state NMR spectroscopy is a powerful analytical tool for characterising non-covalent interactions [1–4], including hydrogen bonding [5] and π–π interactions [6], which direct the arrangement of small and moderately sized organic molecules in the solid state [7]. Specifically, the ^{1}H–^{1}H double-quantum (DQ)/single-quantum (SQ) magic angle spinning (MAS) experiment, first reported in 1994 [8], employs, e.g., the BAck-to-BAck (BABA) [9–11] scheme to recouple the homonuclear ^{1}H–^{1}H dipolar interaction and, as MAS technologies have advanced, has found increasing applications in the field [2,4]. Moreover, the ^{14}N–^{1}H heteronuclear multiple quantum coherence (HMQC) experiment, adapted from the analogous solution-state experiment and reported in the solid state for the first time in 2006 [12,13], is a powerful probe of nitrogen–proton interactions [14–16], and notably hydrogen bonding in, for example, guanosine self-assembly [17,18] and pharmaceuticals [19–21]. These and other two-dimensional ^{1}H MAS experiments e.g. NOESY-like SQ/SQ spin diffusion and ^{13}C–^{1}H heteronuclear correlation experiments, are finding increasing application [22–41].

In such two-dimensional ^{1}H MAS spectra, strong NMR signals due to alkyl protons can lead to excessive t_1 noise, presenting as long trails emanating from that resonance in the solid-state spectra, thus considerably detracting from the appearance and viewability of such spectra as observed, for instance, for nucleic acid derivatives [17]. This phenomenon is caused by relaxation processes induced by the conformational flexibility of those functional groups. Such t_1 noise is frequently observed in solution-state NMR, often as a result of residual proton signal from deuterated solvents, where it is known that the t_1 noise (also referred to as multiplicative noise) is proportional to the signal strength [42]. Processing algorithms for the removal of this noise have been presented, such as Reference Deconvolution [43], the Cadzow procedure [44] or

* Corresponding author.
E-mail address: S.P.Brown@warwick.ac.uk (S.P. Brown).

http://dx.doi.org/10.1016/j.jmr.2015.09.005
1090-7807/

Correlated Trace Denoising [45]. Experimentally, long, weak rf pulses, or selective pulse schemes such as DANTE [46,47] can be applied to saturate offending signals [48], often in combination with pulsed field gradients (PFG), e.g. WATERGATE [49] (WATER suppression by GrAdient-Tailored Excitation). In solid-state NMR, related methods have been presented for the suppression of the water peak in ^{1}H MAS NMR of biological solids [50–53].

Consider the challenge of suppressing t_1 noise due to alkyl side chain resonances, i.e., the case where the nuclear spins that are to be saturated are within the same spin system as those that are of interest. Using a specially adapted PFG MAS probe head, Fischbach et al. demonstrated the applicability of WATERGATE and DANTE based sequences for selectively exciting and suppressing alkyl side chain resonances, applying these sequences to the ^{1}H–^{1}H DQ/SQ MAS experiment [54]. The requirement for specially adapted probe heads means that there has been low uptake of this method; hence there is a motivation to develop alternative approaches applicable with a standard MAS probe head. We show here that slower ^{1}H spin diffusion combined with high resolution at fast MAS frequencies allows for the use of a selective saturation pulse to suppress intense and unwanted signals, while having a less marked effect on the remaining resonances of interest in the spectrum.

Specifically, in this paper, we show that by employing a simple selective pulse prior to the main pulse sequence, and in combination with fast MAS (60+ kHz), it is possible to dramatically improve the appearance of two-dimensional homo- and heteronuclear experiments in the solid state by essentially eliminating or severely reducing the intensity of a strong perturbing signal, hence minimising t_1 noise. The effectiveness of this method is demonstrated using the DNA base analogue 5-iodo-2′-deoxy-3′,5′-di(triisopropylsilyl[TIPS])cytidine [55] henceforth referred to as compound **1** ($C_{27}H_{52}IN_3O_4Si_2$); such pyrimidine (and purine) derivatives have manifold applications in the rapidly evolving area of molecular self-assembly [56–65].

2. Experimental details

2.1. Sample preparation

The DNA base analogue 5-iodo-2′-deoxy-3′,5′-di(triisopropylsilyl) cytidine **1** was prepared according to published methods [55].

2.2. Solid-state NMR experiments

All solid-state NMR experiments were performed at 16.4 T on a JEOL solid-state NMR spectrometer (JEOL ECA700II) operating at a ^{1}H Larmor frequency of 700 MHz and equipped with a 1.0 mm double-resonance Ultrafast MAS probe (JEOL RESONANCE Inc., Tokyo, Japan) with a maximum attainable MAS frequency of 80 kHz; the rotor volume is 0.8 μL corresponding to approximately 0.8 mg of **1**. Except for selective pulses, the ^{1}H $\pi/2$ pulse duration was 0.9 μs. A recycle delay of 3 s was used in all experiments. ^{1}H chemical shifts were referenced with respect to neat TMS using L-alanine as a secondary reference (1.3 ppm for CH_3 ^{1}H resonance, corresponding to 1.85 ppm for adamantane [66]). ^{14}N chemical shifts were referenced relative to neat CH_3NO_2 using the ^{14}N resonance of NH_4Cl (powdered solid) at 341.2 ppm as an external reference (see Table 2 of Ref. [67]. To convert to the chemical shift scale frequently used in protein NMR, where the alternative IUPAC

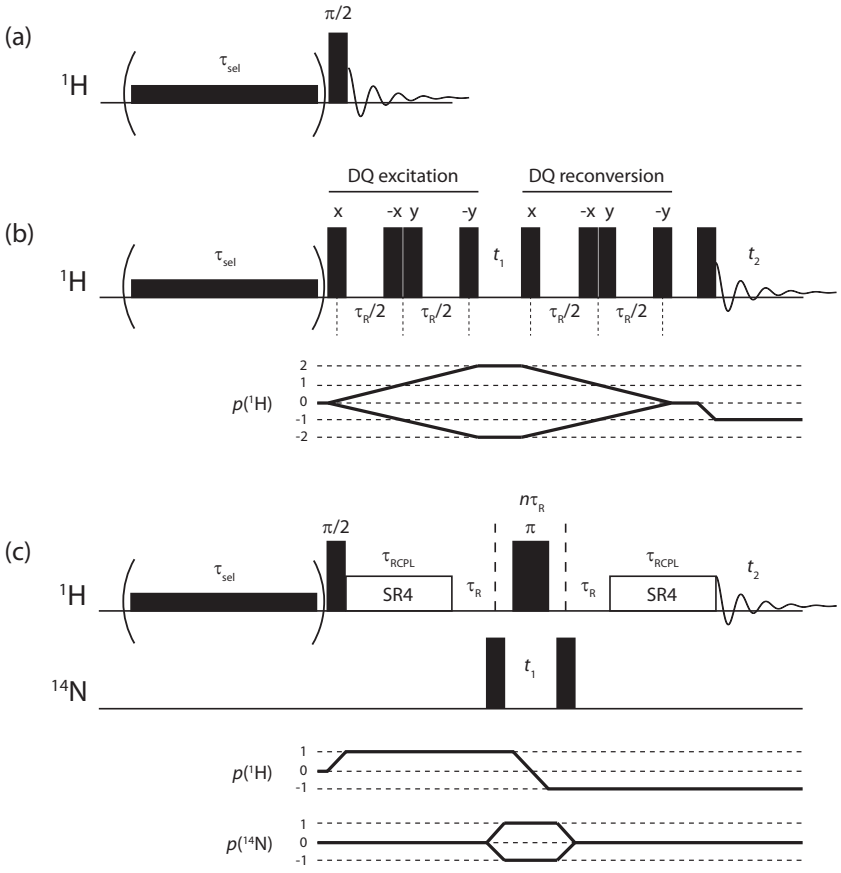

Fig. 1. Schematic representation of pulse sequences with/without selective saturation pulses together with coherence transfer pathways for ^{1}H and ^{14}N for (a) 1D ^{1}H MAS, (b) 2D ^{1}H–^{1}H DQ/SQ MAS (with BABA recoupling) and (c) ^{14}N–^{1}H HMQC (with SR4 recoupling) experiments.

reference (see Appendix 1 of Ref. [68]) is liquid ammonia at 50 °C, it is necessary to add 379.5 to the given values [69]. In all two-dimensional experiments, the States-TPPI method [70] was used to achieve sign discrimination in F_1.

The pulse sequences and coherence transfer pathway diagrams for the experiments incorporating selective saturation pulses are presented in Fig. 1: (a) ^{1}H MAS, (b) ^{1}H–^{1}H DQ/SQ MAS (with BABA recoupling) [9–11] and (c) ^{14}N–^{1}H HMQC (with SR4 recoupling) [71] experiments.

2.2.1. ^{1}H–^{1}H DQ/SQ MAS [2,4] experiments

Eight rotor periods of the BABA-xy16 recoupling sequence [11] ($90 - \tau - 90\ 90 - \tau - 90$, where $\tau = \tau_R/2 - 2 * (90°)_{\text{pulse length}}$) were used for the excitation and reconversion of DQ coherence (for a discussion of the use of different recoupling techniques at fast MAS frequencies, see Ref. [72]). A four-step nested phase cycle [16(0), 16(180), 16(90), 16(270)] can be applied to the selective saturation pulse (there is no change in receiver phase given that the selective pulse is a saturation pulse and not an excitation pulse). A 16-step phase cycle was used to select $\Delta p = \pm 2$ (4-steps) [0, 90, 180, 270] on the BABA-xy16 excitation block and $\Delta p = -1$ (4 steps) [4(0), 4(180), 4(90), 4(270)] on the z-filter $\pi/2$ pulse, where p is the coherence order. The receiver phase was [2(0, 180), 2(180, 0), 2(90, 270), 2(270, 90)]. For each of 64 t_1 FIDs with a rotor synchronised t_1 increment of 29 μs, 16 transients were coadded, corresponding to a total experimental time of 100 min.

2.2.2. ^{1}H–^{1}H NOESY-like spin diffusion experiments [2]

For each of 64 t_1 FIDs with a rotor synchronised t_1 increment of 29 μs, 2 transients were coadded, corresponding to a total experimental time of 12 min. A [0, 180] phase cycle was used to select a change in coherence order $\Delta p = \pm 1$ on the second $\pi/2$ pulse, with the receiver phase following, i.e., [0, 180].

2.2.3. ^{14}N–^{1}H HMQC experiments

SR4 recoupling [71] was used to reintroduce the heteronuclear ^{14}N–^{1}H dipolar couplings, using a duration $\tau_{RCPL} = 171$ μs. The ^{14}N pulse duration was 20 μs. A four-step nested phase cycle [8(0), 8(180), 8(90), 8(270)] was applied to the selective saturation pulse. For the ^{14}N excitation pulse, a two-step phase cycle [0, 180] was employed to select changes in coherence order $\Delta p = \pm 1$. For the ^{1}H $\pi/2$ pulse, the four-step phase cycle [2(0), 2(180), 2(90), 2(270)] was employed. The receiver phase was [0, 2(180), 0, 270, 2(90), 270].

3. One-dimensional ^{1}H MAS NMR spectra

A standard one-pulse ^{1}H MAS spectrum of **1** is presented in Fig. 2. Although there is no published crystal structure available for this compound, related structures are well-known to form hydrogen bonded dimers and the two-dimensional spectra of **1** (presented below) suggest the formation of this motif as shown in Fig. 2. The observation of two peaks for specific chemically distinct sites, notably NHb^{I}/b^{II} at 11.3 and 10.7 ppm, shows that there are two distinct molecules in the asymmetric unit cell. For **1**, the ^{1}H resonance corresponding to the methyl groups contained within the TIPS protecting group is approximately 36 times more intense than the next most intense signal (in terms of peak height), namely that of the ribose sugar group protons at approximately 4.0 ppm. The key resonances, NHa^{I}/a^{II} and NHb^{I}/b^{II}, are over 100 times less intense when compared to the methyl peak height. In terms of integrated intensity, the combined NHb^{I}/NHb^{II} peak is 54 times weaker than the methyl resonance – note that the expected ratio is 42:1 given the relative numbers of protons in each environment. This small deviation arises from the difficulty in assigning

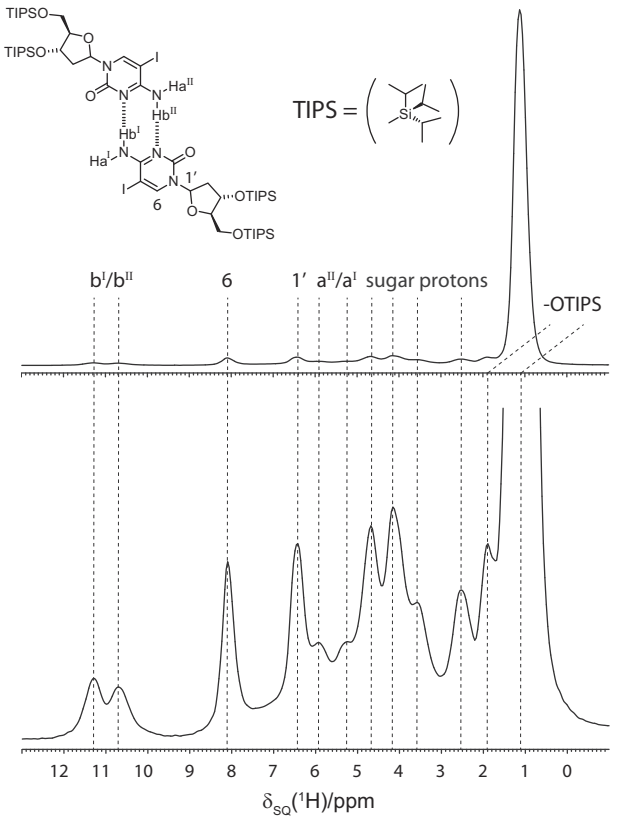

Fig. 2. A ^{1}H (700 MHz) MAS (70 kHz) one-pulse spectrum of **1**. Four transients were coadded with a recycle delay of 3 s. In the lower plot, the intense TIPS methyl resonance at 1.1 ppm has been truncated at approximately 8% of its full height. The spectrum is assigned according to the atomic labels given in the proposed hydrogen bonded dimer arrangement.

integrated intensity for overlapping ^{1}H resonances as well as differences in T_1 relaxation times. The measured T_1 values, determined from a saturation recovery experiment, for the nitrogen bonded protons and the methyl protons show a clear difference: 2.46 and 2.19 s for the NHb^{I} and NHb^{II} protons, respectively, and 0.93 s for the CH_3 resonance. We note that differences in hydrogen T_1 relaxation times under MAS have previously been observed in ^{2}H and ^{1}H studies [73,74].

The effectiveness of a long selective pulse at reducing the signal intensity of a methyl resonance at different MAS frequencies is demonstrated in Fig. 3 for **1**. It is evident that the ^{1}H resolution improves with increasing MAS frequency [75–81]. A comparison of the simple one-pulse ^{1}H MAS spectra (dashed line Fig. 3) and the spectra with a selective saturation pulse with nutation frequency 725 Hz and duration 30 ms (solid line Fig. 3) demonstrate the importance of fast MAS when utilising such selective saturation pulses. It is observed that the key high ppm NHb resonances of interest in **1** are largely unaffected by the use of the selective pulse at all MAS frequencies. By comparison, the signal intensity of the nitrogen bound protons NHa^{II} and NHa^{I} (5.9 and 5.3 ppm) are increasingly suppressed at lower spinning frequencies. This observation highlights the improved effectiveness of selective saturation pulses at fast MAS frequencies (60+ kHz). Note that even at a MAS frequency of 70 kHz, significant loss of signal intensity is observed in the spectral region between 2.0 and 4.0 ppm, resonances which correspond to methylene and ribose sugar group protons. This is, however, not a significant drawback in this particular system since the resonances of interest are the cytidine protons (5.0 ppm and above) which form the important hydrogen bonding interactions and not those of the ribose sugar.

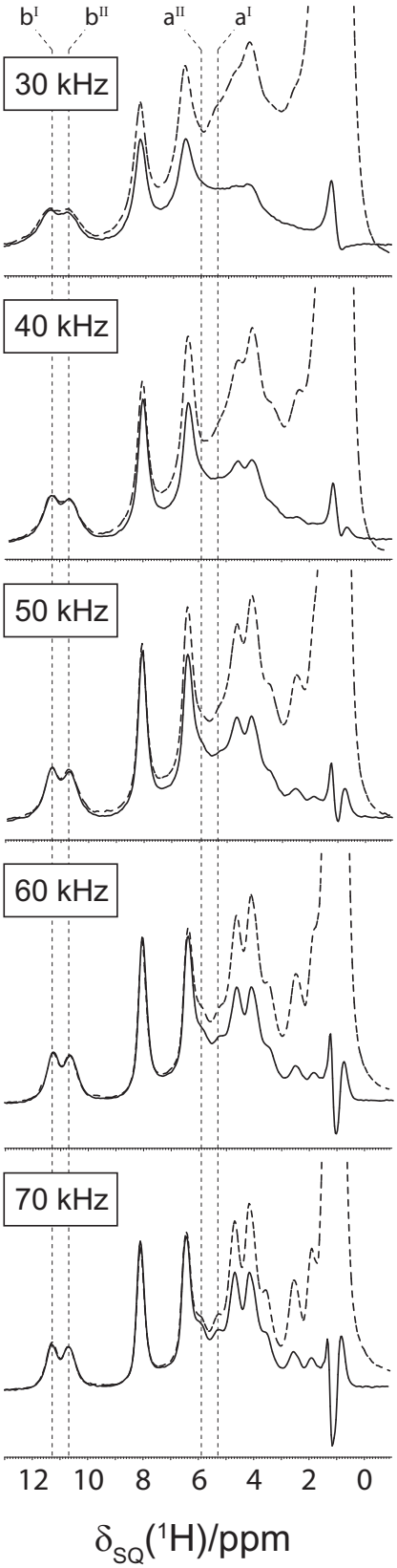

Fig. 3. Comparison of ^{1}H (700 MHz) MAS spectra of **1** obtained at different MAS frequencies. For each spinning frequency, two spectra are shown corresponding to (dashed line) a standard one-pulse ^{1}H MAS spectrum and (solid line) a ^{1}H MAS spectrum acquired utilising a selective saturation pulse (τ_{sel} = 30 ms, with a nutation frequency of 725 Hz). In all cases, 4 transients were coadded with a recycle delay of 3 s.

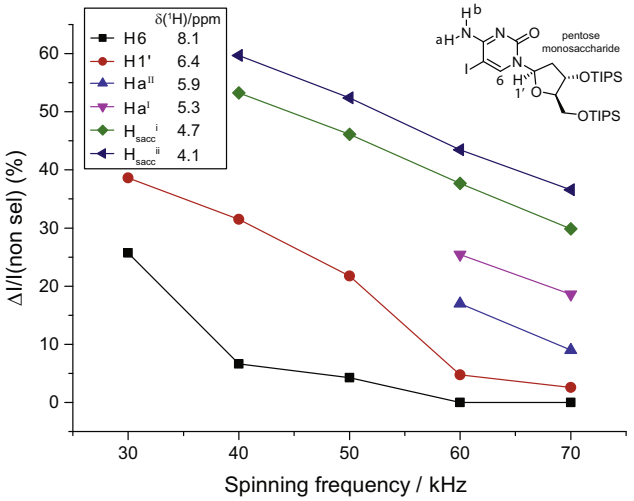

Fig. 4. The signal intensity loss in a ^{1}H MAS one-pulse spectrum of **1** (see Fig. 3) when applying a selective pulse, acquired utilising a selective saturation pulse (τ_{sel} = 30 ms, with a nutation frequency of 725 Hz), as a percentage of the total signal intensity as compared to the case without the selective pulse is shown for six resonances: H6, H1′, NHa^{II}, NHa^{I}, H$^{i}_{sacc}$ and H$^{ii}_{sacc}$, with the corresponding ^{1}H chemical shift values stated in the box. Note that due to insufficient resolution at lower spinning frequencies, some points are omitted from the analysis. Error bars are smaller than the size of the symbols.

For the ^{1}H MAS spectra presented in Fig. 3, the loss of signal intensity when the selective pulse is turned on as a percentage of the total signal intensity, ($\Delta I/I$ (non sel)), is plotted against MAS frequency in Fig. 4 for six resonances: H6, H1′, NHa^{II}, NHa^{I}, H$^{i}_{sacc}$ and H$^{ii}_{sacc}$. The increased loss in intensity at lower MAS frequencies is clearly demonstrated for all six peaks. Note that, due to the reduction in resolution at lower MAS frequencies, it was not possible to resolve either the NHa^{II} or NHa^{I} resonances at 30, 40 or 50 kHz nor the H$^{i}_{sacc}$ and H$^{ii}_{sacc}$ resonances at 30 kHz MAS, and hence these data are omitted from the plot.

Fig. 4 reveals the extent to which signal intensities in the ^{1}H spectra are reduced at lower MAS frequencies when a selective pulse is employed, corresponding to the increased efficiency of ^{1}H spin diffusion at lower spinning frequencies. The signal intensity of the ribose bound protons H$^{i}_{sacc}$ and H$^{ii}_{sacc}$ are reduced significantly even at 70 kHz MAS. There is also a sizable reduction in intensity for the nitrogen bound NHa^{I} and NHa^{II} protons, however this reduction is less than 20% and hence these signals are still clearly evident at this spinning frequency when the selective pulse is applied. MAS frequencies of 60+ kHz are therefore required in order to extract the full benefits of utilising the selective saturation pulse. In this context, it is also to be remembered that resolution becomes worse as the MAS frequency is reduced. Thus two factors, i.e. reduced resolution coupled with the significant reduction in signal intensity for the peaks of interest, effectively precludes the use of this technique at moderate or slow MAS frequencies. In summary, the resolution benefits of fast MAS (60+ kHz), the sensitivity enhancement at higher magnetic fields (700 MHz in this case) and the t_1 noise suppression abilities of the selective saturation pulse combine to render this an attractive technique for multidimensional solid-state NMR experiments. This will be demonstrated for applications to the ^{1}H–^{1}H DQ/SQ MAS and ^{14}N–^{1}H HMQC experiment in Sections 5 and 6.

The choice of a nutation frequency of 725 Hz and a duration of 30 ms for the selective saturation pulse is a compromise between maximising the degree of saturation of the unwanted intense alkyl resonance and minimising the signal reduction for the other nearby (in ppm) ^{1}H resonances of interest. This is illustrated by

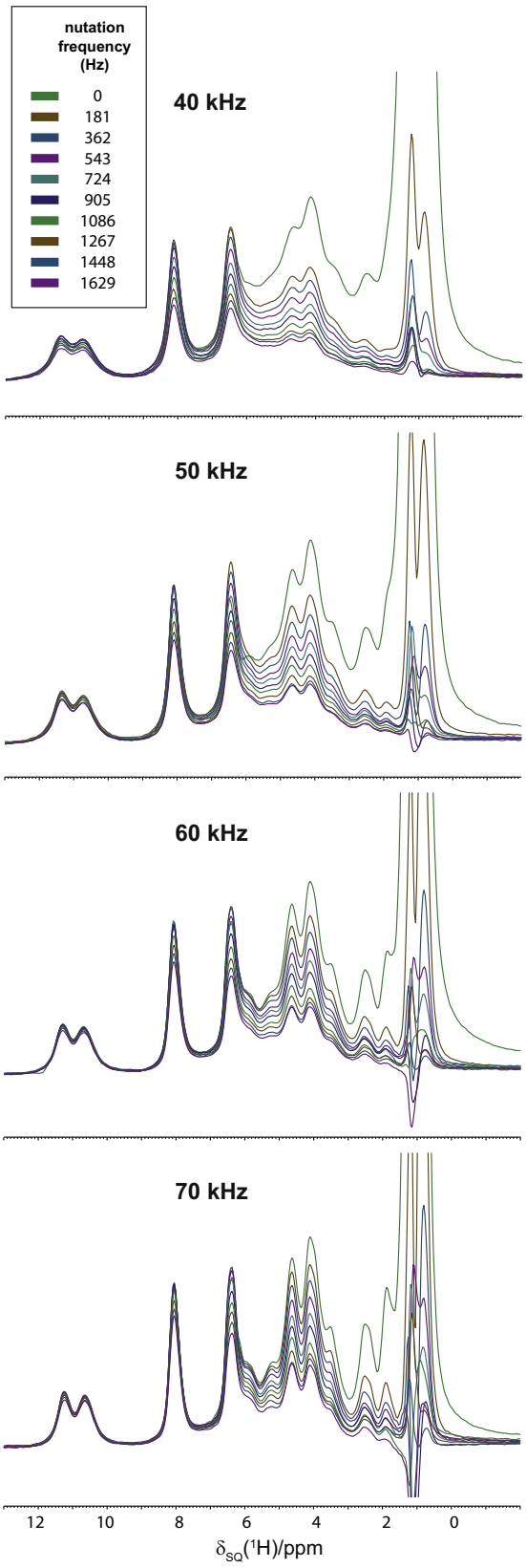

Fig. 5. Comparison of ^{1}H (700 MHz) MAS spectra of **1** obtained at different MAS frequencies. For each spinning frequency, the spectrum obtained using a standard one-pulse ^{1}H MAS experiment is compared to ^{1}H MAS spectra acquired utilising a selective saturation pulse of duration τ_{sel} = 30 ms, but with a varying nutation frequency, as indicated in the inset. In all cases, 4 transients were coadded with a recycle delay of 3 s.

Fig. 5 which shows the effect of changing the nutation frequency for a fixed duration of 30 ms at MAS frequencies of 40, 50 and 60 and 70 kHz. For the intense alkyl resonance, increasing the nutation frequency reduces the signal intensity, with a partial signal inversion and an out-of-phase lineshape being observed at the faster spinning frequencies for the highest nutation frequencies. For the other resonances below 9 ppm, at all MAS frequencies, there is a progressive decrease in intensity upon increasing the nutation frequency, with this observation having been made in the above discussion of Figs. 3 and 4. This phenomenon is a consequence of spin diffusion being reduced at the faster MAS frequencies (see Section 4 below), resulting in less relative reduction of signal intensity for, e.g., the 8 ppm resonance. The two highest ppm resonances show only small decreases in intensity.

Fig. 6 considers the case of a fixed MAS frequency (of 70 kHz) and a fixed nutation frequency of 725 Hz, but allowing the duration of the saturation pulse to increase. Moreover, the top and bottom plots in Fig. 6 compare the case of a saturation pulse with fixed phase and XYXY phase modulation [82], respectively. Analogous trends are seen as in Fig. 5, namely, considering the resonances below 9 ppm (but not the intense alkyl resonance), there is a progressive decrease in intensity upon increasing the saturation pulse duration, while the two highest ppm resonances show only small

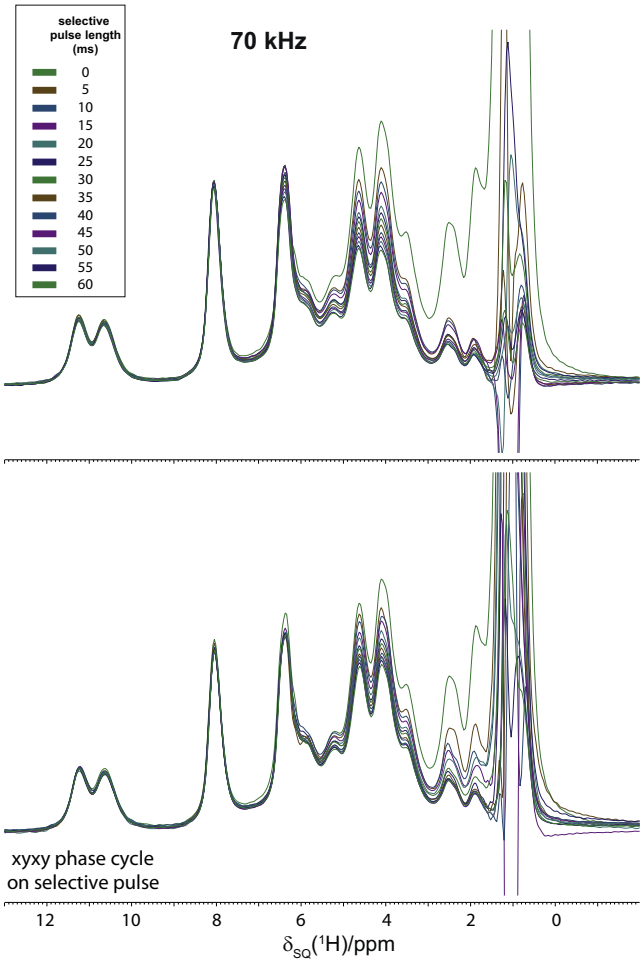

Fig. 6. Comparison of ^{1}H (700 MHz) MAS spectra of **1** obtained at 70 kHz MAS. A spectrum obtained using a standard one-pulse ^{1}H MAS experiment is compared to ^{1}H MAS spectra acquired utilising a selective saturation pulse of nutation frequency 725 Hz and varying duration, as indicated in the inset. For the bottom part, a XYXY phase modulation was applied. In all cases, 4 transients were coadded with a recycle delay of 3 s.

decreases in intensity. Qualitatively, the same trends are observed between the cases of fixed phase and XYXY phase modulation, though the optimum total pulse duration is different.

4. ^{1}H–^{1}H NOESY-like spin-diffusion MAS NMR spectra

In the above section, it has been shown that enhanced performance of the saturation pulse in terms of reduced reduction of intensity for nearby (in ppm) ^{1}H resonances is observed at faster MAS frequencies. This has been explained in terms of reduced efficiency of spin diffusion upon increasing MAS frequency. This is explored further in this section by means of consideration of ^{1}H–^{1}H NOESY-like spin diffusion spectra of **1** recorded with a τ_{mix} = 30 ms at MAS frequencies of 30, 40, 50, 60 and 70 kHz, as presented in Fig. 7. It is evident that cross peak intensity (relative to the auto peaks) is reduced at the faster MAS frequencies. Specifically, Table 1 presents an analysis of peak intensity for the rows at frequencies of 11.3, 10.7, 8.2 and 6.4 ppm, i.e., corresponding to the NHb^{I}, NHb^{II}, H6 and H1′ resonances, respectively. It is evident that some cross peaks that are clearly visible at 30 kHz are at or below the noise level at 70 kHz, for example, cross peaks between NHb^{I} or NHb^{II} and H6 or H1′, i.e., corresponding to longer-range H–H distances as compared to the cross peaks between NHb^{I} and NHb^{II}. This observation is consistent with the Liouville space simulations of ^{1}H spin diffusion at different MAS frequencies as presented in Fig. 4 of Ref. [83]. It is important to note that whilst spin diffusion in this sense is not the same as what happens during the course of rf irradiation [84], such an experiment does appear to act as a good indicator to account for the signal loss observed during a selective saturation pulse experiment. Compared to the ^{1}H–^{1}H DQ/SQ MAS and ^{14}N–^{1}H (700 MHz) HMQC spectra presented below, the t_1 noise associated with the intense alkyl peak has less of a perturbing effect on the appearance of the ^{1}H–^{1}H NOESY-like spin diffusion spectrum; this is presumably a consequence of the reduced relative intensity of the cross peaks in the ^{1}H–^{1}H DQ/SQ MAS and ^{14}N–^{1}H (700 MHz) HMQC spectra.

5. ^{1}H–^{1}H DQ MAS NMR spectra

A ^{1}H–^{1}H (700 MHz) DQ/SQ MAS (70 kHz) spectrum of **1** proves difficult to interpret (Fig. 8b) due to the extent and magnitude of the t_1 noise present in the spectrum; however when a selective saturation pulse is applied prior to the ^{1}H–^{1}H DQ/SQ MAS pulse sequence (see Fig. 1), a remarkable improvement in appearance is observed (Fig. 8c). One-dimensional ^{1}H DQ-filtered spectra (t_1 = 0) of **1** obtained with and without the use of a selective pulse are shown in Fig. 8a. For the spectrum in Fig. 8b, although some information pertaining to the CH_2 resonances is lost, the resonances above 5.0 ppm which correspond to the cytidine protons can now be clearly identified. In this way, it is possible to distinguish several important cross peaks, yielding key information

Table 1
Peak intensities[a] extracted from rows taken from the ^{1}H–^{1}H (700 MHz) NOESY-like spin diffusion spectra in Fig. 7.

	NHb^{I}	NHb^{II}	H6	H1′
30 kHz MAS				
NHb^{I} (11.3 ppm)	**0.25**	0.14	0.63	0.27
NHb^{II} (10.7 ppm)	0.19	**0.09**	0.56	0.29
H6 (8.2 ppm)	0.23	0.14	**2.59**	0.92
H1′ (6.4 ppm)	0.16	0.07	1.33	**0.82**
40 kHz MAS				
NHb^{I} (11.3 ppm)	**0.50**	0.18	0.62	0.09
NHb^{II} (10.7 ppm)	0.36	**0.23**	0.53	0.29
H6 (8.2 ppm)	0.15	0.10	**5.45**	1.23
H1′ (6.4 ppm)	0.23	0.13	1.86	**2.60**
50 kHz MAS				
NHb^{I} (11.3 ppm)	**0.58**	0.43	0.42	0.12
NHb^{II} (10.7 ppm)	0.41	**0.44**	0.39	0.15
H6 (8.2 ppm)	0.21	0.11	**7.45**	0.38
H1′ (6.4 ppm)	0.24	0.08	1.36	**4.62**
60 kHz MAS				
NHb^{I} (11.3 ppm)	**0.82**	0.48	0.28	0.34
NHb^{II} (10.7 ppm)	0.33	**0.74**	0.58	0.33
H6 (8.2 ppm)	0.12	0.08	**7.85**	0.43
H1′ (6.4 ppm)	0.16	0.05	0.93	**6.79**
70 kHz MAS				
NHb^{I} (11.3 ppm)	**0.61**	0.45	0.17	0.17
NHb^{II} (10.7 ppm)	0.21	**1.00**	0.16	–
H6 (8.2 ppm)	0.13	0.09	**13.1**	0.47
H1′ (6.4 ppm)	0.11	–	0.57	**9.19**

[a] Intensities are expressed as percentages of the highest peak (the methyl autopeak) in that spectrum. Integration is performed over the following ranges: NHb^{I}: 12.0–11.0 ppm, NHb^{II}: 11.0–10.0 ppm, H6: 8.7–7.6 ppm, H1′: 6.9–6.1 ppm. Note that bold numbers indicate the integrated intensity of diagonal peaks.

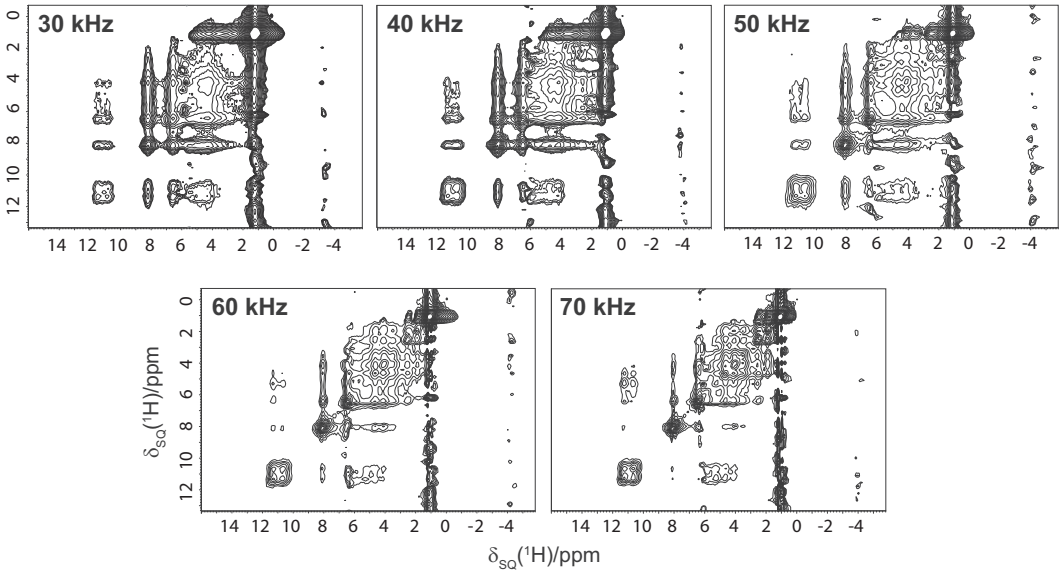

Fig. 7. ^{1}H–^{1}H (700 MHz) NOESY-like spin diffusion spectra of **1** recorded using a mixing time equal to 30 ms at MAS frequencies of 30, 40, 50, 60 and 70 kHz. The base contour level is at 0.05% (30 kHz), 0.03% (40 kHz), 0.02% (50 kHz), 0.02% (60 kHz) and 0.02% (70 kHz) of the maximum peak height.

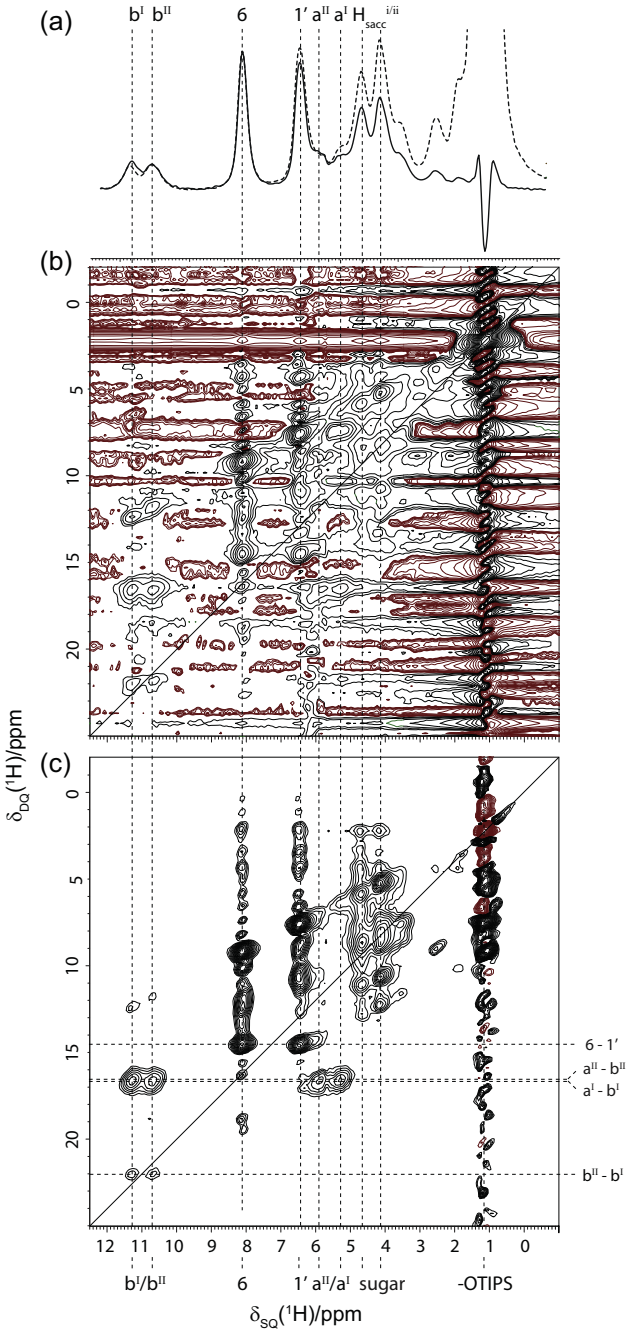

Fig. 8. A comparison of ^{1}H–^{1}H (700 MHz) DQ/SQ MAS (70 kHz) spectra of **1** obtained using the pulse sequence shown in Fig. 1b: (a) 1D (DQ-filtered, i.e., $t_1 = 0$) spectra without a selective pulse (dashed line) and with a selective pulse of nutation frequency 725 Hz and $\tau_{sel} = 30$ ms (solid line), (b and c) 2D spectra obtained (b) without a selective saturation pulse and (c) with a selective pulse of nutation frequency of 725 Hz and duration, $\tau_{sel} = 30$ ms. Eight rotor periods of BABA-xy16 recoupling [9–11] were used for the excitation and reconversion of DQ coherence. The base contour level is at (a) 22% and (b) 3% of the maximum peak height in each spectrum, with negative contours shown in red. (For interpretation of the references to colour in this figure legend, the reader is referred to the web version of this article.)

regarding the molecular packing arrangement (the interpretation of the observed DQ peaks for the supramolecular self-assembly of **1** will be described elsewhere). To quantify the improvement, for the row at DQ frequency of a 22.0 ppm, the integrated intensity of the NHb^{II} peak at 10.7 ppm as a percentage of integrated t_1 noise (in magnitude mode) at the methyl resonance changes from 14% (without a selective pulse, Fig. 8b) to 38% (with a selective pulse, Fig. 8c). The benefits of high magnetic field (700 MHz) and a fast MAS frequency (70 kHz) can clearly be seen, now that the t_1 noise has been largely suppressed in the indirect dimension.

6. ^{14}N–^{1}H HMQC MAS NMR spectra

The efficacy of a selective pulse at reducing t_1 noise is also evident for heteronuclear correlation experiments, such as the ^{14}N–^{1}H HMQC solid-state NMR experiment. In this experiment, it is often useful to observe ^{14}N lineshapes and hence the removal of t_1 noise from the indirect dimension is of considerable importance. One- and two-dimensional ^{14}N–^{1}H HMQC spectra of **1** obtained with and without the use of a selective pulse are shown in Fig. 9.

Inspection of the two 1D ^{14}N–^{1}H HMQC filtered ($t_1 = 0$) spectra of **1** in Fig. 9**a** reveals a sizeable reduction in the intensity of the methyl resonance. This reduction in signal intensity is achieved with minimal loss of intensity for the NH bound protons (and the H6 and H1′ cytidine protons) and leads to a significant improvement in the appearance of the two-dimensional ^{14}N–^{1}H HMQC spectrum in Fig. 7c. In Fig. 9b (standard ^{14}N–^{1}H HMQC experiment), it is difficult to differentiate between 'real' signals and the signals which arise due to the t_1 noise. By contrast, in Fig. 9c, corresponding to the application of a selective pulse, it is possible to clearly observe distinct two-dimensional resonances, including the observation of separate peaks corresponding to the anomeric H1′ proton and that of the NHa protons, thereby aiding spectral assignment. Spectral features due to the aromatic H6 proton at approximately 8.0 ppm are also clearly apparent. To quantify the improvement, for the row at a ^{14}N shift of 100 ppm, the integrated intensity of the NHb^{II} peak at 10.7 ppm as a percentage of integrated t_1 noise (in magnitude mode) at the methyl resonance changes from 5% (without a selective pulse, Fig. 8b) to 20% (with a selective pulse, Fig. 8c).

It has been previously discussed that the performance of the ^{14}N–^{1}H HMQC experiment has a dependence on the MAS frequency: Tatton et al. [16] demonstrated for a β-AspAla dipeptide that good experimental performance is achieved only at frequencies above 45 kHz. Specifically, in addition to improved line narrowing, an increase in ^{1}H coherence lifetimes was also observed (as an increase in integrated signal intensity) upon doubling the MAS frequency from 30 to 60 kHz. While in Ref. [13], rotary resonance recoupling (R^3) at the $n = 2$ condition ($\nu_1 = 2\nu_R$) was employed, Nishiyama and co-workers showed [15] that the same extension of coherence lifetimes was also achieved by using, as employed in this paper, the SR4 recoupling sequence [71]. We note that, as shown in Fig. 3, it is likewise only at spinning frequencies above 40 kHz that the use of a selective saturation pulse becomes feasible.

7. Summary

It has been demonstrated that a single, long, low amplitude selective saturation pulse can be applied to good effect for removing t_1 noise from the indirect dimension of two-dimensional solid-state NMR experiments under fast MAS frequencies (60+ kHz). However, there are several considerations which must be taken into account before employing such methods. The first of these must be the extent of ^{1}H–^{1}H spin diffusion over the duration of the selective pulse. If and when polarisation transfer between different ^{1}H sites becomes apparent the choice of whether to proceed is sample specific. It is therefore important to have some idea of the molecular structure in order to identify valuable resonances. If, as was the case for **1**, these 'resonances of interest' are largely unaffected by spin diffusion over the timescale of the pulse, then this method can improve the presentation and readability of a

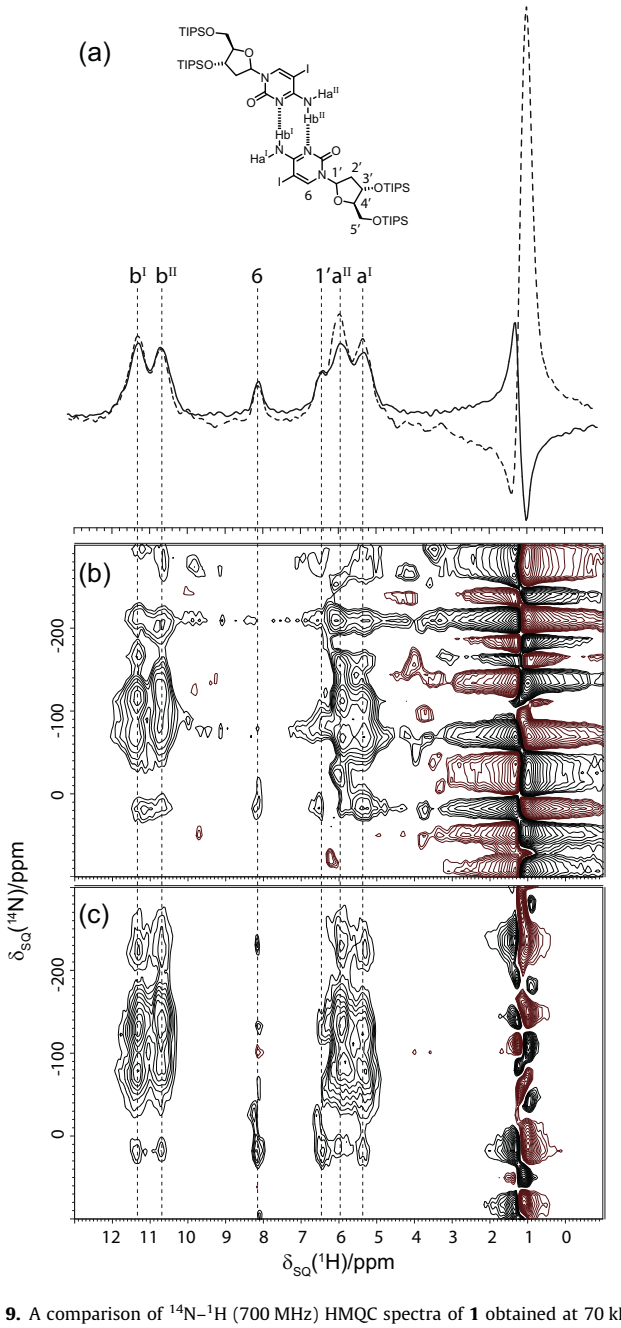

Fig. 9. A comparison of ^{14}N–^{1}H (700 MHz) HMQC spectra of **1** obtained at 70 kHz MAS, using the pulse sequence shown in Fig. 1c (a) 1D (HMQC-filtered, i.e., $t_1 = 0$) spectra without a selective pulse (dashed line) and with a selective pulse of nutation frequency 725 Hz and $\tau_{sel} = 30$ ms (solid line), (b and c) 2D spectra (b) without and (c) with a selective pulse of nutation frequency 725 Hz and $\tau_{sel} = 30$ ms. (b) 128 or (c) 224 transients were recorded for each of the 32 t_1 FIDs, corresponding to experimental times of 7 or 12 h respectively. All spectra were recorded using SR4 recoupling [71] of the ^{14}N–^{1}H heteronuclear dipolar couplings for a $\tau_{RCPL} = 171$ μs. The base contour level is at (b) 42% and (c) 38% of the maximum peak height in each spectrum, with negative contours shown in red. (For interpretation of the references to colour in this figure legend, the reader is referred to the web version of this article.)

spectrum and can, for instance, aid the assignment of DQ peaks corresponding to specific proton proximities (as was the case in Fig. 8).

The second (and equally important) consideration is the availability of fast MAS probes and, to a lesser extent, access to high magnetic fields. Not only does this result in the expected enhancement in both resolution and sensitivity but, as has been demonstrated here, the effect of fast MAS frequencies on the spin dynamics of the system leads to a suppression of magnetisation transfer between different proton environments, hence reducing the loss in signal intensity for all non-intentionally suppressed proton environments. These factors combined generate impressive results in two-dimensional solid-state NMR experiments, as was demonstrated in Figs. 8 and 9, where it was possible to highlight several important contacts and correlations and hence assign the solid state packing arrangement for a DNA base analogue.

In conclusion, we have demonstrated the efficacy of a simple selective saturation pulse at reducing t_1 noise when centred at the offending resonance, which in the case of **1** corresponds to an abundance of methyl moieties contained within the triisopropylsilyl protecting group. This method leads to a much needed reduction in the intensity of such resonances and results in an impressive improvement in two-dimensional ^{1}H–^{1}H DQ/SQ MAS and ^{14}N–^{1}H HMQC spectra. In principle, the approach could be extended to incorporate the application of a doubly-selective pulse, as achieved using a cosine-modulated Gaussian pulse [85–88]. Crucially, this technique requires no specialised apparatus beyond a standard fast spinning probe and therefore represents a simple and accessible tool for the removal of unwanted noise from the indirect dimension of important two-dimensional solid-state NMR spectra. The simplicity of this method should lend itself to the 'everyday' NMR spectroscopist who has an interest in the solid state chemistry of a given material. As fast MAS frequencies become more commonly attainable, the applicability of this technique should increase.

Acknowledgments

We thank EPSRC for funding (PhD studentship to AJR). We also thank scientists from JEOL resonance for their help with the 1.0 mm fast MAS probe. Helpful discussions with Matthias Ernst (ETH Zurich) concerning rf-driven spin diffusion are acknowledged. All experimental NMR data for this study are provided as a supporting dataset from WRAP, the Warwick Research Archive Portal at http://wrap.warwick.ac.uk/71829.

References

[1] S.P. Brown, H.W. Spiess, Chem. Rev. 101 (2001) 4125–4155.
[2] S.P. Brown, Prog. Nucl. Magn. Reson. Spectrosc. 50 (2007) 199–251.
[3] A. Lesage, Phys. Chem. Chem. Phys. 11 (2009) 6876–6891.
[4] S.P. Brown, Solid State Nucl. Magn. Reson. 41 (2012) 1–27.
[5] T. Steiner, Angew. Chem., Int. Ed. Engl. 41 (2002) 48–76.
[6] C.A. Hunter, J.K.M. Sanders, J. Am. Chem. Soc. 112 (1990) 5525–5534.
[7] G.R. Desiraju, Angew. Chem. Int. Ed. 46 (2007) 8342–8356.
[8] H. Geen, J.J. Titman, J. Gottwald, H.W. Spiess, Chem. Phys. Lett. 227 (1994) 79–86.
[9] W. Sommer, J. Gottwald, D.E. Demco, H.W. Spiess, J. Magn. Reson., Ser. A 113 (1995) 131–134.
[10] I. Schnell, A. Lupulescu, S. Hafner, D.E. Demco, H.W. Spiess, J. Magn. Reson. 133 (1998) 61–69.
[11] K. Saalwächter, F. Lange, K. Matyjaszewski, C.-F. Huang, R. Graf, J. Magn. Reson. 212 (2011) 204–215.
[12] S. Cavadini, S. Antonijevic, A. Lupulescu, G. Bodenhausen, J. Magn. Reson. 182 (2006) 168–172.
[13] Z. Gan, J.P. Amoureux, J. Trébosc, Chem. Phys. Lett. 435 (2007) 163–169.
[14] S. Cavadini, Prog. Nucl. Magn. Reson. Spectrosc. 56 (2010) 46–77.
[15] Y. Nishiyama, Y. Endo, T. Nemoto, H. Utsumi, K. Yamauchi, K. Hioka, T. Asakura, J. Magn. Reson. 208 (2011) 44–48.
[16] A.S. Tatton, J.P. Bradley, D. Iuga, S.P. Brown, Z. Phys. Chem. 226 (2012) 1187–1203.
[17] A.L. Webber, S. Masiero, S. Pieraccini, J.C. Burley, A.S. Tatton, D. Iuga, T.N. Pham, G.P. Spada, S.P. Brown, J. Am. Chem. Soc. 133 (2011) 19777–19795.
[18] G.N.M. Reddy, D.S. Cook, D. Iuga, R.I. Walton, A. Marsh, S.P. Brown, Solid State Nucl. Magn. Reson. 65 (2015) 41–48.
[19] A.S. Tatton, T.N. Pham, F.G. Vogt, D. Iuga, A.J. Edwards, S.P. Brown, Cryst. Eng., Commun. 14 (2012) 2654–2659.
[20] K. Maruyoshi, D. Iuga, O.N. Antzutkin, A. Alhalaweh, S.P. Velaga, S.P. Brown, Chem. Commun. 48 (2012) 10844–10846.
[21] A.S. Tatton, T.N. Pham, F.G. Vogt, D. Iuga, A.J. Edwards, S.P. Brown, Mol. Pharmaceut. 10 (2013) 999–1007.

[22] N. Mifsud, B. Elena, C.J. Pickard, A. Lesage, L. Emsley, Phys. Chem. Chem. Phys. 8 (2006) 3418–3422.
[23] T. Schaller, U.P. Büchele, F.-G. Klärner, D. Bläser, R. Boese, S.P. Brown, H.W. Spiess, F. Koziol, J. Kussmann, C. Ochsenfeld, J. Am. Chem. Soc. 129 (2007) 1293–1303.
[24] J.M. Griffin, D.R. Martin, S.P. Brown, Angew. Chem. Int. Ed. 46 (2007) 8036–8038.
[25] A. Brinkmann, V.M. Litvinov, A.P.M. Kentgens, Magn. Reson. Chem. 45 (2007) S231–S246.
[26] E. Salager, R.S. Stein, C.J. Pickard, B. Elena, L. Emsley, Phys. Chem. Chem. Phys. 11 (2009) 2610–2621.
[27] F.G. Vogt, J.S. Clawson, M. Strohmeier, A.J. Edwards, T.N. Pham, S.A. Watson, Cryst. Growth Des. 9 (2009) 921–937.
[28] M. Khan, V. Enkelmann, G. Brunklaus, J. Am. Chem. Soc. 132 (2010) 5254–5263.
[29] T.N. Pham, S.A. Watson, A.J. Edwards, M. Chavda, J.S. Clawson, M. Strohmeier, F. G. Vogt, Mol. Pharmaceut. 7 (2010) 1667–1691.
[30] M. Fritzsche, A. Bohle, D. Dudenko, U. Baumeister, D. Sebastiani, G. Richardt, H. W. Spiess, M.R. Hansen, S. Höger, Angew. Chem. Int. Ed. 50 (2011) 3030–3033.
[31] T. Metzroth, A. Hoffmann, R. Martin-Rapun, M.M.J. Smulders, K. Pieterse, A.R.A. Palmans, J.A.J.M. Vekemans, E.W. Meijer, H.W. Spiess, J. Gauss, Chem. Sci. 2 (2011) 69–76.
[32] J.P. Bradley, S.P. Velaga, O.N. Antzutkin, S.P. Brown, Cryst. Growth Des. 11 (2011) 3463–3471.
[33] L. Mafra, S.M. Santos, R. Siegel, I. Alves, F.A. Almeida Paz, D. Dudenko, H.W. Spiess, J. Am. Chem. Soc. 134 (2012) 71–74.
[34] E. Carignani, S. Borsacchi, J.P. Bradley, S.P. Brown, M. Geppi, J. Phys. Chem. B 117 (2013) 17731–17740.
[35] M.R. Chierotti, R. Gobetto, Cryst. Eng., Commun. 15 (2013) 8599–8612.
[36] D.V. Dudenko, P.A. Williams, C.E. Hughes, O.N. Antzutkin, S.P. Velaga, S.P. Brown, K.D.M. Harris, J. Phys. Chem. B 117 (2013) 12258–12265.
[37] M. Baias, C.M. Widdifield, J.-N. Dumez, H.P.G. Thompson, T.G. Cooper, E. Salager, S. Bassil, R.S. Stein, A. Lesage, G.M. Day, L. Emsley, Phys. Chem. Chem. Phys. 15 (2013) 8069–8080.
[38] M. Sardo, S.M. Santos, A.A. Babaryk, C. López, I. Alkorta, J. Elguero, R.M. Claramunt, L. Mafra, Solid State Nucl. Magn. Reson. 65 (2015) 49–63.
[39] G.M. Peters, L.P. Skala, T.N. Plank, H. Oh, G.N. Manjunatha Reddy, A. Marsh, S.P. Brown, S.R. Raghavan, J.T. Davis, J. Am. Chem. Soc. 137 (2015) 5819–5827.
[40] J. Xu, V.V. Terskikh, Y. Chu, A. Zheng, Y. Huang, Chem. Mater. 27 (2015) 3306–3316.
[41] M. Baias, A. Lesage, S. Aguado, J. Canivet, V. Moizan-Basle, N. Audebrand, D. Farrusseng, L. Emsley, Angew. Chem. Int. Ed. 54 (2015) 5971–5976.
[42] J. Granwehr, Appl. Magn. Reson. 32 (2007) 113–156.
[43] A. Gibbs, G.A. Morris, A.G. Swanson, D. Cowburn, J. Magn. Reson., Ser. A 101 (1993) 351–356.
[44] C. Brissac, T. Malliavin, M. Delsuc, J. Biomol. NMR 6 (1995) 361–365.
[45] S. Poulding, A.J. Charlton, J. Donarski, J.C. Wilson, J. Magn. Reson. 189 (2007) 190–199.
[46] G. Bodenhausen, R. Freeman, G.A. Morris, J. Magn. Reson. 23 (1976) 171–175.
[47] G.A. Morris, R. Freeman, J. Magn. Reson. 29 (1978) 433–462.
[48] R. Freeman, Chem. Rev. 91 (1991) 1397–1412.
[49] M. Piotto, V. Saudek, V. Sklenář, J. Biomol. NMR 2 (1992) 661–665.
[50] V. Chevelkov, B.J. van Rossum, F. Castellani, K. Rehbein, A. Diehl, M. Hohwy, S. Steuernagel, F. Engelke, H. Oschkinat, B. Reif, J. Am. Chem. Soc. 125 (2003) 7788–7789.
[51] E.K. Paulson, C.R. Morcombe, V. Gaponenko, B. Dancheck, R.A. Byrd, K.W. Zilm, J. Am. Chem. Soc. 125 (2003) 15831–15836.
[52] D.H. Zhou, C.M. Rienstra, J. Magn. Reson. 192 (2008) 167–172.
[53] J.R. Lewandowski, J.-N. Dumez, Ü. Akbey, S. Lange, L. Emsley, H. Oschkinat, J. Phys. Chem. Lett. 2 (2011) 2205–2211.
[54] I. Fischbach, K. Thieme, A. Hoffmann, M. Hehn, I. Schnell, J. Magn. Reson. 165 (2003) 102–115.
[55] A. Marsh, N.W. Alcock, W. Errington, R. Sagar, Tetrahedron 59 (2003) 5595–5601.
[56] T. Torring, N.V. Voigt, J. Nangreave, H. Yan, K.V. Gothelf, Chem. Soc. Rev. 40 (2011) 5636–5646.
[57] J. Shimada, T. Maruyama, M. Kitaoka, H. Yoshinaga, K. Nakano, N. Kamiya, M. Goto, Chem. Commun. 48 (2012) 6226–6228.
[58] A. Kuzyk, R. Schreiber, Z. Fan, G. Pardatscher, E.-M. Roller, A. Hogele, F.C. Simmel, A.O. Govorov, T. Liedl, Nature 483 (2012) 311–314.
[59] Y. Zhang, F. Lu, K.G. Yager, D. van der Lelie, O. Gang, Nat. Nano 8 (2013) 865–872.
[60] S.K. Albert, H.V.P. Thelu, M. Golla, N. Krishnan, S. Chaudhary, R. Varghese, Angew. Chem. Int. Ed. 53 (2014) 8352–8357.
[61] C. Tian, X. Li, Z. Liu, W. Jiang, G. Wang, C. Mao, Angew. Chem. 126 (2014) 8179–8182.
[62] M.-Q. Zhao, Q. Zhang, G.-L. Tian, F. Wei, Nanoscale 6 (2014) 9339–9354.
[63] Y. Li, Z. Liu, G. Yu, W. Jiang, C. Mao, J. Am. Chem. Soc. 137 (2015) 4320–4323.
[64] L. Cademartiri, K.J.M. Bishop, Nat. Mater. 14 (2015) 2–9.
[65] J. Li, C. Zheng, S. Cansiz, C. Wu, J. Xu, C. Cui, Y. Liu, W. Hou, Y. Wang, L. Zhang, I. t. Teng, H.-H. Yang, W. Tan, J. Am. Chem. Soc. 137 (2015) 1412–1415.
[66] S. Hayashi, K. Hayamizu, Bull. Chem. Soc. Jpn. 64 (1991) 685–687.
[67] S. Hayashi, K. Hayamizu, Bull. Chem. Soc. Jpn. 64 (1991) 688–690.
[68] R.K. Harris, E.D. Becker, S.M.C. De Menezes, P. Granger, R.E. Hoffman, K.W. Zilm, Pure Appl. Chem. 80 (2008) 59–84.
[69] G.E. Martin, C.E. Hadden, J. Nat. Prod. 63 (2000) 543–585.
[70] D. Marion, M. Ikura, R. Tschudin, A. Bax, J. Magn. Reson. 85 (1989) 393–399.
[71] A. Brinkmann, A.P.M. Kentgens, J. Am. Chem. Soc. 128 (2006) 14758–14759.
[72] B. Hu, Q. Wang, O. Lafon, J. Trébosc, F. Deng, J.P. Amoureux, J. Magn. Reson. 198 (2009) 41–48.
[73] M. Cutajar, M.H. Lewis, S. Wimperis, Chem. Phys. Lett. 449 (2007) 86–91.
[74] J.J. Kweon, R. Fu, J.A. Kitchen, P.L. Gor'kov, W.W. Brey, N.S. Dalal, J. Phys. Chem. C 119 (2015) 5013–5019.
[75] I. Schnell, S.P. Brown, H.Y. Low, H. Ishida, H.W. Spiess, J. Am. Chem. Soc. 120 (1998) 11784–11795.
[76] I. Schnell, H.W. Spiess, J. Magn. Reson. 151 (2001) 153–227.
[77] A. Samoson, T. Tuherm, Z. Gan, Solid State Nucl. Magn. Reson. 20 (2001) 130–136.
[78] V.E. Zorin, S.P. Brown, P. Hodgkinson, J. Phys. Chem. 125 (2006) 144508.
[79] T. Kobayashi, K. Mao, P. Paluch, A. Nowak-Król, J. Sniechowska, Y. Nishiyama, D.T. Gryko, M.J. Potrzebowski, M. Pruski, Angew. Chem. Int. Ed. 52 (2013) 14108–14111.
[80] V. Agarwal, S. Penzel, K. Szekely, R. Cadalbert, E. Testori, A. Oss, J. Past, A. Samoson, M. Ernst, A. Böckmann, B.H. Meier, Angew. Chem. Int. Ed. 53 (2014) 12253–12256.
[81] J.M. Lamley, D. Iuga, C. Öster, H.-J. Sass, M. Rogowski, A. Oss, J. Past, A. Reinhold, S. Grzesiek, A. Samoson, J.R. Lewandowski, J. Am. Chem. Soc. 136 (2014) 16800–16806.
[82] Y. Ishii, J.P. Yesinowski, R. Tycko, J. Am. Chem. Soc. 123 (2001) 2921–2922.
[83] J.-N. Dumez, M.C. Butler, L. Emsley, J. Phys. Chem. 133 (2010) 224501.
[84] P. Robyr, B.H. Meier, R.R. Ernst, Chem. Phys. Lett. 162 (1989) 417–423.
[85] L. Emsley, I. Burghardt, G. Bodenhausen, J. Magn. Reson. 90 (1990) 214–220.
[86] X. Miao, R. Freeman, J. Magn. Reson., Ser. A 119 (1996) 90–100.
[87] S. Cadars, A. Lesage, N. Hedin, B.F. Chmelka, L. Emsley, J. Phys. Chem. B 110 (2006) 16982–16991.
[88] G. Pileio, S. Mamone, G. Mollica, I.M. Montesinos, A. Gansmüller, M. Carravetta, S.P. Brown, M.H. Levitt, Chem. Phys. Lett. 456 (2008) 116–121.